

Quantitative study of the interdependence of interface structure and giant magnetoresistance in polycrystalline Fe/Cr superlattices

R. Schad*

*Laboratorium voor Vast-Stoffysika en Magnetisme, Katholieke Universiteit Leuven, B-3001 Leuven, Belgium
and Research Institute for Materials, KU Nijmegen, NL-6525 ED Nijmegen, The Netherlands*

P. Beliën,[†] G. Verbanck, and C. D. Potter

Laboratorium voor Vast-Stoffysika en Magnetisme, Katholieke Universiteit Leuven, B-3001 Leuven, Belgium

H. Fischer

Institute Laue Langevin, 38042 Grenoble Cedex 9, France

S. Lefebvre and M. Bessiere

LURE, Université de Paris-Sud, 91405 Orsay Cedex, France

V. V. Moshchalkov and Y. Bruynseraede

Laboratorium voor Vast-Stoffysika en Magnetisme, Katholieke Universiteit Leuven, B-3001 Leuven, Belgium

(Received 15 September 1997)

We present a quantitative characterization of the interface roughness of Fe/Cr superlattices based on specular and off-specular x-ray diffraction using anomalous scattering. We discuss the dependence of the amplitude of the giant magnetoresistance (GMR) effect, including changes in the interlayer magnetic coupling, on the interface structure. We observe a reduction of the GMR effect with increasing amplitude of the interface roughness having constant lateral correlation length. However, the physical interpretation of this clear result in terms of spin-dependent interface scattering remains unclear because of the unknown bulk contribution. [S0163-1829(98)03918-6]

INTRODUCTION

The discovery of giant magnetoresistance¹ (GMR) in Fe/Cr superlattices opened a new field of possible applications for artificially tailored materials. The effect is explained by spin-dependent scattering of the electrons at impurities or interfaces.²⁻⁴ This spin dependence results from spin-dependent electron states and from the spin dependence of the scattering potential. For instance, the majority electrons of Fe are much stronger scattered at Cr impurities than are the minority electrons.⁵ This leads to different resistivities for the parallel and the antiparallel alignment of the magnetization directions of the magnetic layers. The antiparallel configuration at zero strength of the external field is provided by antiferromagnetic exchange coupling for an appropriate thickness of the Cr spacer layer. This configuration can be forced into parallel alignment by an external field, thus resulting in a change of the resistance. However, antiferromagnetic exchange coupling is not a prerequisite for the observation of the GMR effect since the antiparallel alignment can be obtained also by other methods.^{6,7}

The burning question was and still is, how the size of the GMR effect is related to the structural properties of the superlattice. Here one has to distinguish between several contributions to the GMR which are directly or indirectly linked to the structural properties. These are contributions of (i) the magnetic structure, (ii) the spin-dependent electronic structure, and (iii) the spin-dependent electron scattering.

The magnetic structure is of importance because the full size of the GMR effect is only observed when the magnetic

configuration changes from fully antiparallel to parallel alignment. The latter will be easily achieved only if the external magnetic field is strong enough to saturate the magnetization. The antiferromagnetic alignment at zero field, however, depends (in the case of an exchange coupled superlattice) on the kind of the exchange coupling and on superlattice imperfections in the form of pinholes. Instead of a simple antiferromagnetic alignment, the magnetization directions can form 90° angles between adjacent magnetic layers.⁸ This will reduce the observed GMR by a factor of 2.⁹ The strength of the 90° coupling is mediated by roughness of the interfaces¹⁰ or loose spins inside the spacer layers.¹¹ So, in both cases the 90° coupling indirectly links the size of the GMR effect to the superlattice quality. Magnetic pinholes will cause ferromagnetic alignment of parts of the sample which consequently do not contribute to the GMR effect, thus diminishing its amplitude. Not only pinholes but also precursors of these in the form of larger spacer layer thickness fluctuations might lead to partially ferromagnetic alignment because of local changes of the exchange coupling. These magnetic contributions can be separated experimentally from the pure electronic contributions by magnetization measurements which give directly the fraction of the sample which is antiferromagnetically ordered (AFF) and the part which does not contribute (local ferromagnetic alignment, pinholes) or which contributes only partially to the GMR (angle between magnetization directions of adjacent magnetic layers between 0° and 180°).

The second contribution to the GMR effect, the electronic structure, can generate a GMR effect even in defect-free

point contacts with ballistic transport¹² or in the limit of diluted scatterers.^{13,14} This contribution comes mostly from the asymmetry of the Fermi velocities of the two spin channels. These band-structure effects are to some extent related to the third contribution to the GMR effect, the spin-dependent electron scattering. On one hand, the minigaps in the band structure caused by the periodicity of the superlattice will be influenced by the defects which cause the scattering. On the other hand, the spin dependence of the scattering process is caused by the asymmetry of the band structure, first via the density of states at the Fermi level, and second via the spin-dependent scattering potential at impurities or interfaces. The first contribution makes any scattering event spin dependent, even scattering at phonons.¹⁵ Experimentally, the contributions of the electronic structure and the spin-dependent scattering cannot yet be separated since scattering is dominant in all reported samples so far. It is this spin-dependent scattering that generally receives the most attention in the literature, experimentally and theoretically.

Here two contributions have to be considered separately, the spin-dependent scattering at impurities inside the magnetic layers (referred to as bulk scattering) and the scattering at the interfaces. Both can (in principle) cause a GMR effect.^{16–22} In combination they can even cancel each other provided that their spin asymmetry is opposite. The ideally pure cases, samples with only bulk or only interface scattering, are difficult to achieve experimentally. This would require the growth of samples with either ideally flat interfaces or defect-free layers. However, recent experiments on Co/Cu superlattices indicate that spin-dependent interface scattering dominates the GMR effect.²³

We therefore have a strong motivation to investigate quantitatively the effects of interface structure (e.g., roughness) on GMR. A detailed comparison with theory requires a comprehensive and quantitative analysis of the interface structure. The most powerful technique for this purpose is x-ray diffraction²⁴ (XRD) because, first, it is a nondestructive technique applied after the completion of the growth of the sample, second it probes the whole superlattice structure as it is seen by the electrons in the transport measurements and, third, it uses waves with a wavelength similar to the one of the electrons at the Fermi level of usual metals. Unfortunately, ordinary XRD provides only low contrast for Fe/Cr superlattices, because of the comparable electron densities of Fe and Cr. This effect has impeded until now the quantitative evaluation of the XRD spectra. However, synchrotron radiation allows the use of anomalous diffraction by choosing the wavelength close to the absorption edge of one of the atomic species, resulting in an enhanced contrast. Additionally, recent developments of theoretical models describing specular and diffuse x-ray scattering from superlattices^{25–31} allow simulations of XRD spectra which are characterized by a high degree of agreement with the measured spectra and accordingly deliver very reliable values for the interface structure of the superlattices.

In this paper we present the interpretation of the transport properties of polycrystalline Fe/Cr superlattices based on a quantitative analysis of their XRD data. The transport properties are characterized by high values of the GMR effect (up to 80% for samples with 10 bilayers) indicating the dominance of spin-dependent scattering processes above spin-

independent ones. We present XRD spectra of high quality Fe/Cr superlattices together with simulations which determine the values of parameters for the interface structure both perpendicular to and in the plane of the interfaces.

EXPERIMENTAL

The superlattices were prepared in a Riber molecular-beam epitaxy deposition system (2×10^{-11} mbar base pressure) using electron-beam evaporation hearths, which were rate stabilized to within 1% by a homemade feedback control system³² using Balzers quadrupole mass spectrometers (QMS). Additionally, integration of the QMS signal was used for automatic control of the shutters of the individual evaporation sources. In this way, a reproducible bilayer thickness throughout the whole superlattice was ensured, as well as a constant Cr thickness over all superlattices. The Fe and Cr layers (starting material of 99.996% purity) were electron-beam evaporated in a pressure of 4×10^{-10} mbar at a rate of 1 Å/s on polycrystalline yttrium stabilized zirconium oxide (YSZ) substrates (typically 5×5 mm²). In order to minimize thickness inhomogeneities, the substrate was rotated at 60 rpm during the whole growth process. The surface roughness of the YSZ substrates was evaluated *ex situ* by atomic-force microscopy (AFM). Typical rms values of the YSZ surface roughness were 5 Å on a 1 μm² area. After rinsing in isopropyl alcohol and drying in a dry N₂ flow, the substrate was annealed for 15 min at 600 °C in UHV.

The superlattices consisted of ten bilayers with 22 Å of Fe and 13 Å of Cr starting the growth with a Fe layer. The interface roughness was varied by growing the samples either directly onto the YSZ substrates (sample numbers 5,7,9) or onto a 20 Å thick Cr buffer (sample numbers 6,8,10,12,14,16) using substrate temperatures (TG) increasing from 0 to 400 °C in steps of 50 °C (increasing sample numbers). In this way, we obtained a series of 18 Fe/Cr superlattices of which nine have been selected for this analysis because of their magnetic properties (see below).

The structural characterization of the superlattices was obtained through small angle (SA) XRD measurements using either a synchrotron source with wavelength of 2.0753 Å (15 eV below the Cr absorption edge) or a Rigaku rotating anode diffractometer at 4 kW power and with an x-ray wavelength of 1.542 Å (Cu Kα). The following experimental XRD setups were used: (i) specular reflectivity measurements (or symmetrical ω - 2θ scans) at SA were used to determine the interface roughness η in perpendicular direction; (ii) rocking curve or ω -scan measurements at SA providing information about the lateral correlation length ξ_x of the interface roughness and the Hurst parameter h . The lateral correlation length is a measure for the spatial decay of the height-height correlation function whereas h describes the fractality of the interface structure; (iii) offset $(\omega + \delta) - 2\theta$ scans to study the correlation of the interface roughness in perpendicular direction expressed by the correlation length ξ_z . The measured spectra were simulated applying recently developed theories describing specular as well as diffuse x-ray scattering at superlattices. In this model the scattered intensity is calculated by dynamical scattering in the distorted-wave Born approximation as a function of the vertical and lateral scattering vectors (q_z and q_x). Further details can be found in the origi-

nal literature.^{25–31} Large-angle XRD which usually can be employed for quantitative analysis of the interface structure of superlattices²⁴ cannot be used in this case because the samples are polycrystalline with only poor texture.²⁰ But also in the case of high-quality epitaxial Fe/Cr superlattices^{33,34} the similar lattice constants of Fe and Cr are responsible for the much less pronounced large-angle spectra compared to the SA XRD scans. Therefore, the analysis of the SA data generally delivers more robust values of η .

The electrical measurements were performed in an Oxford cryostat (1.5 up to 300 K) equipped with a 15 T magnet. Resistivities were determined using a standard four-probe Van der Pauw method. The magnetoresistance is defined as $\Delta\rho/\rho_s = (\rho_0 - \rho_s)/\rho_s$, where ρ_0 is the resistivity in zero field and ρ_s the saturation resistivity in a magnetic field H_s parallel to the interfaces. All quoted resistivity values were measured at 4.2 K.

The magnetization measurements were performed in an alternating gradient magnetometer. The antiferromagnetic fraction of the samples is defined as $AFF = 1 - (M_r/M_s)$ with M_r and M_s being, respectively, the remnant and the saturation magnetization. This AFF was used to correct the magnetoresistance for small variations in the magnetic order of the samples by dividing $\Delta\rho$ by AFF.³⁵ This way the magnetoresistance data become independent of this contribution.

RESULTS AND DISCUSSION

As a function of the sample growth temperature TG we found the best layering quality and a maximum of the GMR amplitude around TG=250 °C.²⁰ However, the reduction of the GMR towards higher TG is only caused by a decrease of the AFF (Ref. 35) and is thus a magnetic contribution. Therefore our analysis is restricted to nine samples grown at lower TG where the changes of the GMR are of spin-dependent origin.

First, we will discuss the structural properties of the superlattices measured with XRD. In Ref. 20 we assessed the interface quality by the peak to background intensity ratio of SA XRD rocking curves. This was, however, revealing no information over the lateral roughness length scale and additionally, the intuitive interpretation of the diffuse intensity can be misleading.^{30,31} Here we are able to present a quantitative simulation of the specular and diffuse XRD spectra giving a comprehensive overview over the relevant interface structure parameters. Since not all samples could be measured at the synchrotron source we first will compare simulations of the specular SA XRD data obtained using, respectively, the synchrotron source and the laboratory source. This is demonstrated for the sample with the most pronounced superlattice structure since here any deviations between simulation and measurement will become most obvious, but of course, similar agreement is found also for the other samples (Fig. 1). The specular data show a rich structure being the pronounced superlattice Bragg peaks and the higher frequent finite-size peaks. We produced the best simulation for the spectrum measured at the synchrotron using as input parameters the thicknesses of all layers (Fe, Cr, and a top oxide layer),³⁶ the number of bilayers, the optical parameters of Fe, Cr, YSZ, top oxide,³⁷ and the roughnesses of, respectively, the substrate (determined by AFM) and the top

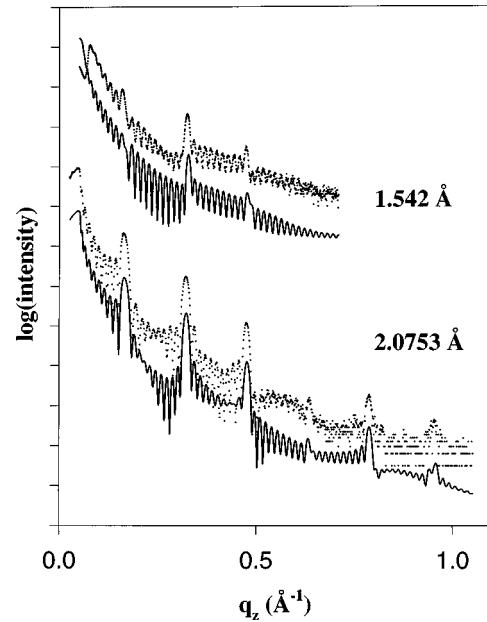


FIG. 1. Specular SA XRD spectra of one sample measured with x-ray wavelengths of, respectively, 1.542 Å (Cu $K\alpha$ laboratory source) and 2.0753 Å (synchrotron source). Shown are the measured data (points) and the simulations (lines). The two simulations are obtained using identical input parameters except for the different optical constants which were taken from literature. All curves are vertically offset for clarity.

oxide. Then the simulation was optimized by adjusting the vertical interface roughness η (Fig. 1 lower curve). The criteria for assessing the quality of a simulation was the matching of the superlattice Bragg peak intensities and shapes. The uncertainty of the obtained roughness value depends on the distinctness of the superlattice structure in the spectrum. This varies with the roughness itself and the x-ray wavelength used. Careful estimates of these uncertainties were obtained by studies of the influence of η on the quality of the simulations and are used as error bars in Fig. 4.

Simulations taking into account possible variations of the interface roughness throughout the stacking of the superlattice (cumulative roughness²⁴ or inequality of Fe/Cr and Cr/Fe interfaces) were not successful so that we can conclude that this effect must be small or absent. In order to keep the number of simulation parameters limited we used identical roughness for all superlattice interfaces. Additionally, it should be noted that the obtained values of η were not influenced by a later fine adjustment of the substrate roughness η_s which only determines the inter-Bragg peak intensity and the damping of the finite-size peak oscillations. We find values of η_s (about 3 Å) being slightly smaller than the ones measured by AFM (about 5 Å). This small difference might be caused by the different lateral length scale over which the two methods are sensitive³⁸ and by the fact that the AFM data were taken in air.

As next step, all parameters of this simulation had served as input parameters for the simulation of the spectrum measured with the Cu $K\alpha$ wavelength. Only the optical constants had, of course, to be changed according to the different wavelength used.³⁷ Although the two measured spectra look very different because of the enhanced material contrast in the case of the synchrotron data for which the wavelength

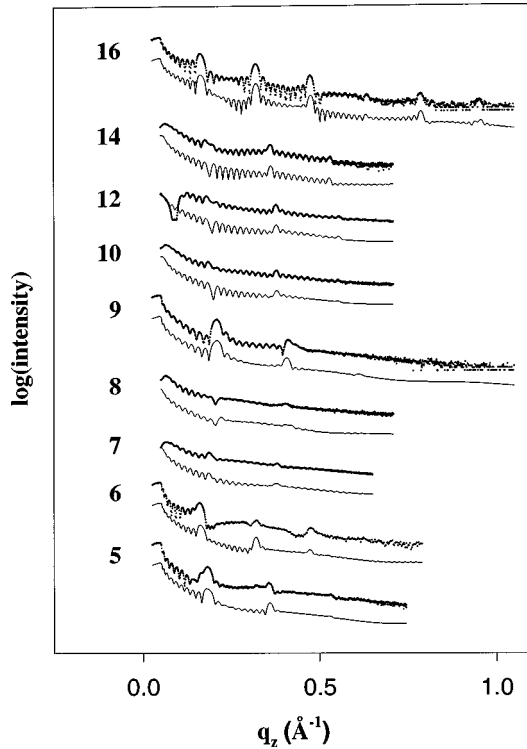


FIG. 2. Specular SA XRD spectra of all samples measured either with a wavelength of 1.542 \AA (Cu $K\alpha$ laboratory source; samples 7, 8, 10, 12, 14) or 2.0753 \AA (synchrotron source; samples 5, 6, 9, 16). Shown are the measured data (crosses) and the simulations (lines). All curves are vertically offset for clarity.

was chosen close to the absorption edge of Cr, both simulations are in excellent agreement with the data (Fig. 1). This degree of agreement proves that spectra from superlattices with such low material contrast as Fe/Cr can be successfully simulated and quantitative roughness data can be obtained. Furthermore, it gives confidence in the structure analysis obtained through simulations of spectra measured with the laboratory source.

The specular data with their respective simulations of all samples are shown in Fig. 2. Deviations between simulation and measurement can be observed at very small angles for all samples measured with the laboratory source (sample numbers 7, 8, 10, 12, 14). This is caused by the nonlinearity of the x-ray detector at high intensities. The other samples had been measured at the synchrotron. Deviations in intensity between measurement and simulation at wave vectors in-between superlattice Bragg peaks (most pronounced in the spectrum of sample 6) are likely caused by surface contamination. In principle, these long-wavelength deviations can be reproduced in the simulation by introducing an extra surface layer of several nm thickness and adjusting its optical parameters. However, this does not influence the intensities of the superlattice Bragg peaks and hence the values obtained for the relevant interface roughness parameter η . Furthermore, this contamination layer is also unlikely to influence the electrical transport data. Therefore, we decided to keep the simulations as simple as possible, only including the relevant layers. In general, the films grown on the Cr buffer are smoother than without buffer. Obviously, this Cr seed layer provides a better template for the superlattice growth than the bare YSZ

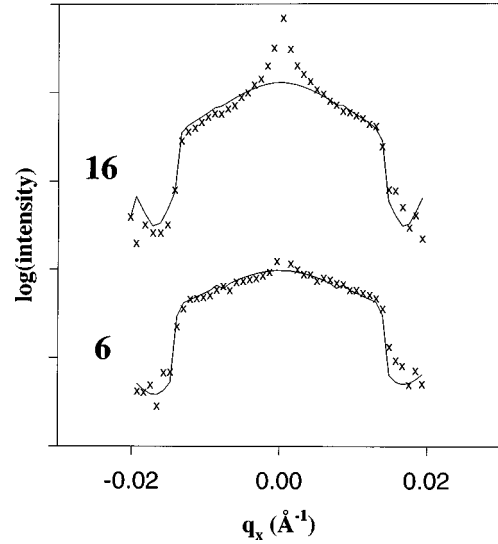


FIG. 3. SA XRD rocking curves of samples 6 and 16 with q_z at the position of the second-order superlattice Bragg peak. Shown are the measured data (crosses) and the simulations (lines). All curves are vertically offset for clarity.

substrate. The η values we obtain are in qualitative agreement with the peak-to-background intensity ratios derived in Ref. 20. However, the quantitative structure analysis by simulation provides values of well-defined structure parameters and additionally, allows us to estimate the lateral roughness components.

The lateral correlation of the interface roughness was measured by ω scans at q_z , the vertical wave vector, set to the position of the second superlattice Bragg peak. These measurements were done at the synchrotron, so data are available for samples 5, 6, 9, and 16 which are samples grown at, respectively, low and high TG and with or without a Cr buffer. Two examples of measured data together with their respective simulation are shown in Fig. 3. The relevant parameters of the simulation are the lateral correlation length ξ_x and the Hurst parameter h which describe the decay of the height-height correlation function. In simple terms h can be taken as a measure for the jaggedness of the interfaces.²⁸ Both parameters will be relevant for the transport properties since, for a given value of the roughness amplitude, they will determine the density of steps at the interfaces which form finally the deviations from a perfect interface, i.e., the scattering centers.³⁹ The interdependence of ξ_x and h results in some uncertainty of their estimated values with $h = 0.5 \pm 0.2$. In order to limit the number of free simulation parameters we kept h fixed at $h = 0.5$. The lateral correlation length is about 90 \AA for all samples. The roughness correlation in the z direction, expressed by ξ_z , is likely of less direct importance for the electron scattering, but it might have an influence on the interlayer exchange coupling via thickness variations of the Cr layer. Variations of the exchange coupling are taken into account by the antiferromagnetic fraction. The samples discussed here have a constant value of $\xi_z = 130 \text{ \AA}$, obtained from simulations of the asymmetric $(\omega + \delta) - 2\theta$ scans.

In summary, the SA XRD analysis reveals that the structural parameters of the samples discussed here vary mostly in the amplitude of the interface roughness ($2.2 \text{ \AA} \leq \eta \leq 5 \text{ \AA}$),

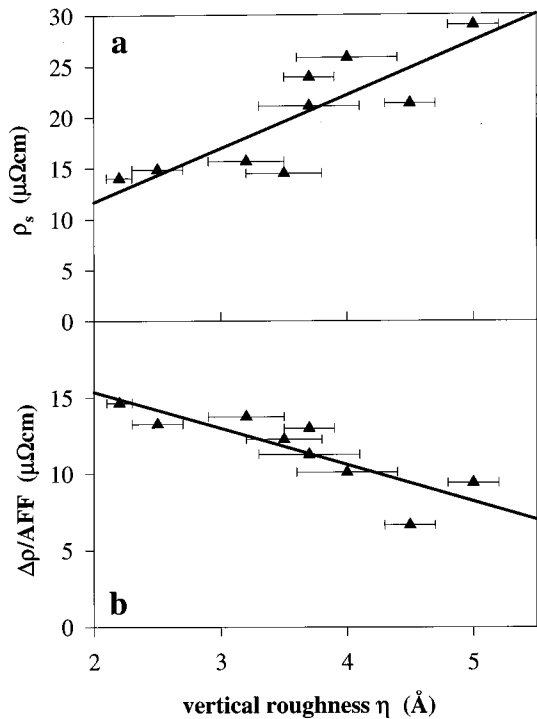


FIG. 4. Saturation resistivity ρ_s (a) and magnetoresistance, corrected for variations of the antiferromagnetic fraction, $\Delta\rho/\text{AFFT}$ (b) as a function of the interface roughness amplitude η . Shown are the measured data (crosses) and linear best fits (lines). ρ_s increases with increasing η whereas $\Delta\rho$ decreases.

with little variation in the lateral roughness parameters. This structural information is now used to understand the transport properties. Since the interface roughness amplitude η is the structure parameter varying mostly we focus on the discussion of ρ_s and $\Delta\rho$ as a function of η (Fig. 4). First, it has to be noted that the GMR $\Delta\rho/\rho_s$ is rather high (up to 80%) compared to values usually reported for nonepitaxial samples.^{16–19} This indicates, in our case, that the spin-dependent electron scattering ($\Delta\rho$) dominates the spin-independent (ρ_s) events. Therefore our analysis is rather independent of uncharacterized changes in structural defects affecting the spin-independent background resistivity. In addition, the transport properties show a strong variation with η indicating a strong link between interface roughness and magnetoresistance. We observe an increase of ρ_s and a decrease of $\Delta\rho$ or $\Delta\rho/\rho_s$ with increasing η (Fig. 4). The explanation of this might be one of the following scenarios:

(i) Neglecting any spin-dependent bulk scattering, the observed roughness dependence of the magnetoresistance has to be ascribed to the changes in the interface properties in the following way. The increasing interface roughness amplitude reduces the spin asymmetry of the interface scattering. This is expected for higher values of η when the minority electrons are also increasingly scattered, thus reducing the spin asymmetry of the interface scattering.⁴ On the other hand, the pronounced superlattice Bragg peaks in the SA XRD spectra indicate rather smooth interfaces, certainly for the best samples. However, the exact value of the roughness amplitude above which the GMR amplitude should decrease with increasing η is not known. An alternative explanation could be the possible occurrence of bigger steps at the interfaces of these polycrystalline superlattices (contrary to epi-

taxial samples). The scattering at such big steps could be less spin selective than at monoatomic ones.

(ii) Since these polycrystalline samples have a high degree of bulk defects it is doubtful whether their contribution can be neglected. Including in the discussion bulk scattering which might have a spin asymmetry in the electron scattering there would exist a GMR effect already without any interface contribution. In order to explain now the observed roughness dependence of the GMR amplitude, the spin asymmetry of the electron scattering at the interfaces would have to be opposite to the bulk contribution. Then increasing scattering at the interfaces increasingly compensates the GMR effect stemming from the bulk scattering. The electrons which are less scattered at the bulk impurities would be scattered at the interfaces and vice versa.⁴

For both scenarios increasing values of η would increase ρ_s and, at the same time, decrease $\Delta\rho$. However, the interface roughness dependence of the spin asymmetry of the interface scattering would be exactly opposite. This dilemma in the interpretation of the experimental data is an inherent problem for all samples with a non-negligible amount of bulk defects, in particular polycrystalline samples. A clear interpretation is impeded not only by the presence of such bulk defects but also their undefined contribution to the spin asymmetry of the electron scattering and their unknown changes in concentration and influence when varying the interface quality. These undefined and variable bulk contributions might also account for the scatter of the transport data in Fig. 4.

SUMMARY

We presented the interpretation of the transport properties of Fe/Cr superlattices based on their structural properties. The GMR effect reaches very high values compared to other polycrystalline samples of up to 80% for ten bilayers indicating the importance of spin-dependent scattering processes. We analyzed the structure of the high-quality Fe/Cr superlattices by quantitative simulation of the XRD spectra revealing the relevant structural interface parameters perpendicular to and in the plane of the interfaces. We found a decrease of the magnetoresistance $\Delta\rho$ and $\Delta\rho/\rho_s$ with increasing roughness amplitude. The theoretical understanding is not clear. The decrease of the magnetoresistance could be either caused by enhanced roughness increasingly scattering electrons of both spin orientations with similar strength or by a compensation of a bulk contribution by the interface scattering having opposite spin asymmetry to the electron scattering. Therefore, a clear experimental result about the influence of the interface structure on the GMR amplitude will have to be based on samples with negligible bulk scattering.

ACKNOWLEDGMENTS

This work was financially supported by the Belgian Concerted Action (GOA) and Interuniversity Attraction Poles (IUAP) programs. R.S., C.D.P., and G.V. acknowledge support by, respectively, the European Community (Marie Curie), the Research Council of the Katholieke Universiteit Leuven, and the Belgium Interuniversity Institute for Nuclear Sciences. We are indebted to J. Barnas for helpful discussion and carefully reading the manuscript.

- * Author to whom correspondence should be addressed: Research Institute for Materials, Katholieke Universiteit Nijmegen, Toernooiveld 1, NL 6525 ED Nijmegen, The Netherlands, Fax +31 (0)24 3652190. Electronic mail: schad@sci.kun.nl
- [†] Present address: Philips Optical Storage, Kempische Steenweg 293, 3500 Hasselt, Belgium.
- ¹ M. N. Baibich, J. M. Broto, A. Fert, F. Nguyen Van Dau, F. Petroff, P. Etienne, G. Creuzet, A. Friederich, and J. Chazelas, *Phys. Rev. Lett.* **61**, 2472 (1988).
- ² R. Q. Hood, L. M. Falicov, and D. R. Penn, *Phys. Rev. B* **49**, 368 (1994).
- ³ Y. Asano, A. Oguria, and S. Maekawa, *Phys. Rev. B* **48**, 6192 (1993).
- ⁴ J. Barnas and Y. Bruynseraede, *Phys. Rev. B* **53**, 5449 (1996).
- ⁵ I. A. Campbell and A. Fert, in *Ferromagnetic Materials*, edited by E. P. Wohlfarth (North-Holland, Amsterdam, 1982).
- ⁶ J. Barnas, A. Fuss, R. E. Camley, P. Grünberg, and W. Zinn, *Phys. Rev. B* **42**, 8110 (1990).
- ⁷ J. Barnas, A. Fuss, R. E. Camley, U. Walz, P. Grünberg, and W. Zinn, *Vacuum* **41**, 1241 (1990).
- ⁸ M. Rührig, R. Schäfer, A. Huber, R. Mosler, J. A. Wolf, S. Demokritov, and P. Grünberg, *Phys. Status Solidi A* **125**, 635 (1991).
- ⁹ C. D. Potter, R. Schad, P. Beliën, G. Verbanck, V. V. Moshchalkov, Y. Bruynseraede, M. Schäfer, R. Schäfer, and P. Grünberg, *Phys. Rev. B* **49**, 16 055 (1994); R. Schad, C. D. Potter, P. Beliën, G. Verbanck, V. V. Moshchalkov, Y. Bruynseraede, M. Schäfer, R. Schäfer, and P. Grünberg, *J. Appl. Phys.* **76**, 6604 (1994).
- ¹⁰ J. C. Slonczewski, *Phys. Rev. Lett.* **67**, 3172 (1991).
- ¹¹ J. C. Slonczewski, *J. Appl. Phys.* **73**, 5975 (1993).
- ¹² Kees M. Schep, Paul J. Kelly, and Gerrit E. W. Bauer, *Phys. Rev. Lett.* **74**, 586 (1995).
- ¹³ P. Zahn, I. Mertig, M. Richter, and H. Eschrig, *Phys. Rev. Lett.* **75**, 2996 (1995).
- ¹⁴ I. Mertig, P. Zahn, M. Richter, H. Eschrig, R. Zeller, and P. H. Dederichs, *J. Magn. Magn. Mater.* **151**, 363 (1996).
- ¹⁵ C. T. Yu, K. Westerholt, K. Theis-Bröhl, and H. Zabel, *J. Appl. Phys.* **82**, 5560 (1997).
- ¹⁶ E. E. Fullerton, D. M. Kelly, J. Guimpel, I. K. Schuller, and Y. Bruynseraede, *Phys. Rev. Lett.* **68**, 859 (1992).
- ¹⁷ N. M. Rensing, A. P. Payne, and B. M. Clemens, *J. Magn. Magn. Mater.* **121**, 436 (1993).
- ¹⁸ N. M. Rensing, B. M. Clemens, and D. L. Williamson, *J. Appl. Phys.* **79**, 7757 (1996).
- ¹⁹ S. Joo, Y. Obi, K. Takahashi, and H. Fujimori, *J. Magn. Magn. Mater.* **104**, 1753 (1992).
- ²⁰ P. Beliën, R. Schad, C. D. Potter, G. Verbanck, V. V. Moshchalkov, and Y. Bruynseraede, *Phys. Rev. B* **50**, 9957 (1994).
- ²¹ J. M. Colino, I. K. Schuller, R. Schad, C. D. Potter, P. Beliën, G. Verbanck, V. V. Moshchalkov, and Y. Bruynseraede, *Phys. Rev. B* **53**, 766 (1996).
- ²² J. M. Colino, I. K. Schuller, V. Korenivski, and K. V. Rao, *Phys. Rev. B* **54**, 13 030 (1996).
- ²³ H. J. M. Swagten, G. J. Strijkers, G. L. J. Verschueren, M. M. H. Willekens, and W. J. M. de Jonge, *J. Magn. Magn. Mater.* **176**, 169 (1997).
- ²⁴ E. E. Fullerton, I. K. Schuller, H. Vanderstraeten, and Y. Bruynseraede, *Phys. Rev. B* **45**, 9292 (1992).
- ²⁵ S. K. Sinha, E. B. Sirota, S. Garoff, and H. B. Stanley, *Phys. Rev. B* **38**, 2297 (1988).
- ²⁶ V. Holý, J. Kubeňka, I. Ohídal, K. Lischka, and W. Poltz, *Phys. Rev. B* **47**, 15 896 (1993).
- ²⁷ V. Holý and T. Baumbach, *Phys. Rev. B* **49**, 10 668 (1994).
- ²⁸ J.-P. Schlomka, M. Tolan, L. Schwalowsky, O. H. Seeck, J. Stettner, and W. Press, *Phys. Rev. B* **51**, 2311 (1995).
- ²⁹ H. E. Fischer, H. Fischer, O. Durand, O. Pellegrino, S. Andrieu, M. Picuch, S. Lefebvre, and M. Bessiere, *Nucl. Instrum. Methods Phys. Res. B* **97**, 402 (1995).
- ³⁰ H. E. Fischer, H. M. Fischer, and M. Picuch (unpublished).
- ³¹ Henry E. Fischer, memoire DHDR (Diplome d'Habilitation a Diriger les Recherches), Universite Joseph Fourier, Grenoble, France.
- ³² W. Sevenhans, J.-P. Locquet, and Y. Bruynseraede, *Rev. Sci. Instrum.* **57**, 937 (1986).
- ³³ E. E. Fullerton, M. J. Conover, J. E. Mattson, C. H. Sowers, and S. D. Bader, *Appl. Phys. Lett.* **63**, 1699 (1993).
- ³⁴ R. Schad, C. D. Potter, P. Beliën, G. Verbanck, V. V. Moshchalkov, and Y. Bruynseraede, *Appl. Phys. Lett.* **64**, 3500 (1994).
- ³⁵ R. Schad, J. Barnas, P. Beliën, G. Verbanck, C. D. Potter, H. Fischer, S. Lefebvre, M. Bessiere, V. V. Moshchalkov, and Y. Bruynseraede, *J. Magn. Magn. Mater.* **156**, 339 (1996).
- ³⁶ The properties of the top oxide layer (typical thickness, roughness, composition, and optical parameters) were characterized in independent experiments [R. Schad, D. Bahr, J. Falta, G. Materlik, P. Beliën, G. Verbanck, K. Temst, and Y. Bruynseraede, *J. Phys. Condens. Matter* **10**, 61 (1998)].
- ³⁷ S. Brennan and P. L. Cowan, *Rev. Sci. Instrum.* **63**, 850 (1992).
- ³⁸ K. Temst, M. J. Van Bael, B. Wuyts, C. van Haesendonck, Y. Bruynseraede, D. G. de Groot, N. Koeman, and R. Griessen, *Appl. Phys. Lett.* **67**, 3429 (1995).
- ³⁹ A. Kaserer and E. Gerlach, *Z. Phys. B* **97**, 139 (1995).